Bioprocess Biosyst Eng (2013) 36:1871–1878
DOI 10.1007/s00449-013-0961-z

ORIGINAL PAPER

Fabrication of a circular PDMS microchannel for constructing a three-dimensional endothelial cell layer

Jong Seob Choi · Yunxian Piao · Tae Seok Seo

Received: 27 March 2013 / Accepted: 23 April 2013 / Published online: 14 May 2013

Abstract We describe a simple and efficient fabrication method for generating microfluidic channels with a circular cross-sectional geometry by exploiting the reflow phenomenon of a thick positive photoresist. Initial rectangular shaped positive photoresist micropatterns on a silicon wafer, which were fabricated by a conventional photolithography process, were converted into a half-circular shape by tuning the temperature to around 105 °C. Through optimization of the reflow conditions, we could obtain a perfect circular micropattern of the positive photoresist, and control the diameter in a range from 100 to 400 μm. The resultant convex half-circular photoresist was used as a template for fabricating a concave polydimethylsiloxane (PDMS) through a replica molding process, and a circular PDMS microchannel was produced by bonding two half-circular PDMS layers. A variety of channel dimensions and patterns can be easily prepared, including straight, S-curve, X-, Y-, and T-shapes to mimic an in vivo vascular network. To form an endothelial cell layer, we cultured primary human umbilical vein endothelial cells inside circular PDMS microchannels, and demonstrated successful cell adhesion, proliferation, and alignment along the channel.

J. S. Choi and Y. Piao contributed equally to the work.

Electronic supplementary material The online version of this article (doi:10.1007/s00449-013-0961-z) contains supplementary material, which is available to authorized users.

J. S. Choi · Y. Piao · T. S. Seo (✉)
Department of Chemical and Biomolecular Engineering and Institute for the BioCentury, Korea Advanced Institute of Science and Technology (KAIST), 291 Daehak-ro, Yuseong-gu, Daejeon 305-701, Republic of Korea
e-mail: seots@kaist.ac.kr

Keywords Polydimethylsiloxane · Circular microchannels · Cell culture · Reflow of photoresist · Human umbilical vein endothelial cells

Introduction

The application of microfabrication technology has expanded from simple biomolecular separation to more complicated genomic, proteomic, and cellular analyses [1]. In particular, the ability of microtechnology for precise control of time and space in microenvironments provides an excellent platform for cell biology and tissue engineering [2, 3]. Microfluidic-based biomimetic devices have demonstrated more reliable and high-throughput drug screening capability compared with the conventional static 2-D cell culture system [4–6]. Research on the construction of an artificial microvascular system on a chip is a good example. Vascular endothelial cells lining the lumina of all blood vessels play an important role in maintaining the homeostasis of the circulatory system, and they are involved in a number of vascular diseases such as atherosclerosis and thrombosis. Study on the vascular endothelium, cardiovascular disease-related functions, and assessment of vascular toxicity in drug screening requires realistic in vitro vascular models [7–10]. The microfabrication technology can provide a vascular microcirculation system including arterioles (250 μm > diameter ≥ 8 μm), capillaries (diameter < 8 μm), and venules (250 μm > diameter ≥ 8 μm) mimicking the organizational complexity of in vivo blood vessel architectures [11].

To this end, many efforts have focused on the fabrication of three-dimensional (3D) microfluidic channels to provide an artificial microvascular system. The most widely accepted fabrication method is based on soft

lithography or molding techniques in numerous polymeric substrates [12, 13]. However, SU-8 negative photoresist template and metal mold-based stamping methods typically generate square, rectangular or trapezoidal cross-sectional shapes in the microchannels or require an expensive metal mold for the stamping and casting processes [14]. Considering that the cross-sectional shape of a microchannel determines fluidic dynamics such as shear stress on the endothelium layer, which affects functional phenotype, gene expression, and cell adhesion, the fabrication of a perfect circular microfluidic channel is crucial to mimic the microvascular model. Moreover, the non-circular microchannel causes difficulties in stable cell seeding at the corners, preventing uniform formation of a confluent endothelial cell layer. It also leads to dead volume, resulting in inefficient circulation of nutrients and oxygen during the cell culture [15].

To overcome such limitations, 3D circular microchannel structures in silicon wafers and polymer scaffolds have been reported. These structures have been obtained by use of an isotropic etching method on glass materials [16], embedment of circular optical fibers into a photoresist [17], and the formation of a bell-shaped microchannel by backside exposure [18]. Wang et al. [15] presented a circular polydimethylsiloxane (PDMS) microfluidic channel by melting a negative photoresist, and Wilson et al. [19] used a metal mold-based mechanical micromilling technique to produce a 1-mm-diameter circular channel. Song et al. [20] presented a microchannel with a near-perfect circular cross-section by removing the circular wire in the PDMS layer. Fiddes et al. [21] developed a circular cross-sectional microchip by introducing N_2 gas into the PDMS solution. Lee et al. [22] showed a directly molded circular microchannel in PMMA by solvent-assisted molding. To date, most fabricated circular channels do not, however, have a perfect shape and require a relatively complicated process. They are also limited in terms of controllability over the diameter of the circular microchannel. In addition, only a few reports on the primary human umbilical vein endothelial cell (HUVEC) culture inside the circular microchannel, an important biological application to mimic the human microvascular scaffold, have been presented.

Here, we present a simple and efficient microfabrication method to produce perfectly circular cross-sectional microchannels by combining a soft lithography method with the reflow phenomenon of a positive photoresist. Since a wide range of thickness of a rectangular positive photoresist can be turned into a circular shape by the reflow technique, we could generate circular PDMS microfluidic channels with diameters from 100 to 400 μm, as well as various channel designs. Furthermore, we have demonstrated a successful primary HUVEC culture in the circular PDMS microchannels to mimic an artificial blood vessel system.

Materials and methods

Chemicals and reagents

All chemicals and reagents were used without further purification or modification. AZ 40XT-11D (positive photoresist) and MIF-300 developer were purchased from AZ Electronic Materials USA Corporation (USA). A <100> Si wafer was obtained from iTASCO (Korea), and hexamethyldisilazane (HMDS) was ordered from Sigma Aldrich. A PDMS prepolymer and a curing agent (Sylgard 184 elastomer kit) were purchased from Dow Corning Corporation (USA). Primary HUVEC and an endothelial growth medium (EGM) bullet kit, which contains an endothelial cell basal medium (EBM) and EGM SingleQuots™ (supplements and growth factors), were purchased from Lonza (San Diego). Triton X-100, 10 % neutral buffered formalin, phalloidin and tetramethylrhodamine B isothiocyanate (TRITC) conjugate, and 4′,6′-diamidino-2-phenylindole (DAPI) were purchased from Sigma (USA). A LIVE/DEAD® viability/cytotoxicity assay kit was obtained from Molecular Probes, Invitrogen (USA).

Fabrication of a circular PDMS microchannel by using a reflow phenomenon

Figure 1 shows the fabrication scheme for the circular microchannels by using soft lithography combined with a reflow phenomenon of a thick positive photoresist. The surface of a Si wafer was treated with HMDS for 1 h to render the surface hydrophobic. A positive photoresist was spin-coated on the Si wafer at 1,000 rpm for 30 s, and the solvent was evaporated for 1 h. A three-stage baking step was then followed at 70 °C for 5 min, 90 °C for 5 min, and 115 °C for 5 min. To increase the height, the photoresist was spin-coated again to form a double layer of resist, which was baked by the same procedure as above (Fig. 1a). To pattern the rectangular shape, the double layered positive photoresist on the Si wafer was exposed to UV-light for 80 s, post-baked at 100 °C for 30 s, and developed in MIF-300 developer with gentle shaking (Fig. 1b). To form the circular patterns, the rectangular shaped positive photoresist was heated at 105 °C for 5 min to lead to the reflow phenomenon, converting the rectangular shape to a circular shape (Fig. 1c). After treatment of HMDS for 1 h, a PDMS prepolymer and PDMS curing agent, mixed at a volume ratio of 10:1, were poured into the convex half-circular photoresist on a Si wafer, and cured in an oven at 65 °C for 12 h (Fig. 1d). The cured PDMS was then carefully peeled off from the Si wafer, and the resultant PDMS microchannel shape was a concave circle (Fig. 1e). Two half-circular PDMS layers were exposed to O_2 plasma for 2 min to generate hydroxyl groups and oxygen radicals on the

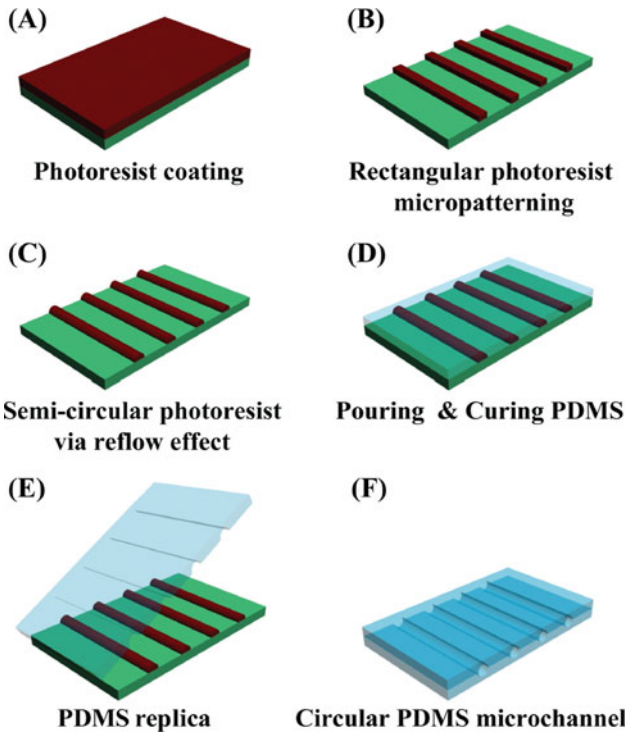

Fig. 1 Fabrication scheme for circular PDMS microchannels by combining reflow phenomenon of a thick positive photoresist and soft lithography

surface, and then permanently bonded to produce a nearly perfect circular PDMS microchannel (Fig. 1f). The channel dimensions were controlled by tuning the thickness of the positive photoresist, and various shaped microchannels, such as straight, S-curve, X-, Y-, and T-shapes, were generated through the photomask designs.

HUVEC culture in the circular PDMS microchannel

HUVECs of passage number 2–4 were cultured in an EGM containing an EBM, EGM SingleQuots™ (supplements and growth factors), and 1 % antibiotics. The cells were grown in a humidified 5 % CO_2 incubator at 37 °C. After confluency, the cells were trypsinized with 0.25 % trypsin and 0.05 % EDTA (Gibco, Invitrogen, USA) for 3 min, and then concentrated by centrifugation and resuspended with the complete medium to adjust the cell concentration to 2×10^6 cell/mL. The circular PDMS microfluidic channel (diameter of 250 μm) was sterilized with 70 % ethanol and exposed to UV overnight. The surface of the circular microchannel was coated with 0.1 mg/mL fibronectin by incubation at 37 °C for 1 h. After washing with Dulbecco's phosphate-buffered saline (DPBS; Gibco, Invitrogen, USA), the harvested HUVECs were introduced into the microchannel by using a micro-syringe pump with a flow rate of 14 nL/s. After 10 min incubation in a humidified 5 % CO_2 incubator at 37 °C for cell attachment, the circular PDMS microchannel was turned upside down, and similar amounts of HUVECs were introduced again. After another incubation period of 2 h for complete and stable cell adhesion inside the entire circular microchannel, the chip was immersed in a petri dish containing a static media solution, which prevented any possibility of cell detachment or bubble formation during the cell culture. To monitor the time-course cell growth profiles, the microdevice in the petri dish was put into a miniaturized incubator (Live Cell Instrument, Korea), and fluorescence cell images were recorded with a phase contrast microscope (Nikon, ECLIPSE, TE 2000-U). The process of the HUVEC culture in the half-circular microchannel was similar as that described above except that 10 μL of cell stock solution (2×10^6 cell/mL) was loaded onto the fibronectin-coated microchannel.

Cell fluorescence staining and live/dead cell assay

For immunostaining, HUVECs were fixed by using 10 % of neutral buffered formalin and permeabilized with 0.1 % of Triton X-100. Cells were stained for filamentous actins and nuclei using 50 μg/mL of TRITC-conjugated phalloidin (Sigma, USA) and 1 μg/mL of DOPI (Sigma, USA), respectively. These staining reagents were introduced into the HUVEC cultured microchannel at a flow rate of 14 nL/s. A live/dead cell assay was conducted after a 3-day culture in the circular PDMS microchannel by using calcein-AM and ethidium homodimer-1 for live and dead cell imaging. Before staining, the serum containing media and the unbound cells were washed out by infusion of DPBS for 5 min, and then a solution containing calcein-AM (2 μM) and ethidium homodimer-1 (4 μM) was injected into the microchannel at a flow rate of 14 nL/s for 5 min. After incubation at 37 °C for 30 min, the green fluorescence from live cells and the red fluorescence from dead cells were visualized under a confocal laser microscope (Nikon, D-ECLIPSE, C1si). To view the 3D HUVEC in the circular microchannel, the z-stack (0.5-mm spacing) images were recorded. To test the stable HUVEC attachment on the surface under high shear stress conditions, the cultured cells in the microchannel were exposed to a flow of 14 μL/s for 2 h.

Scanning electron microscope (SEM) images of the HUVECs in the circular microchannel

The surface morphology of HUVECs in the circular microchannel or a flat surface was analyzed by scanning electron microscope (SEM, Hitachi S-4800, Japan). Briefly, after cultured for 3 days, the cells were washed with PBS, followed by fixation with 4 % glutaraldehyde (GA, Sigma) for 1 h at room temperature. After GA was

thoroughly washed out with distilled water, the fixed cells were sequentially immerged in ethanol solutions of 30, 40, 50, 60, 70, 80, 90 and 100 % with incubation time of 10 min. Finally, the remaining ethanol was evaporated at room temperature with ambient air, and the dried sample was coated with a thin layer of gold–palladium, which was then ready for the SEM analysis.

Results and discussion

Fabrication of circular shape in a thick positive photoresist by using reflow phenomenon

The reflow phenomenon of a positive photoresist is illustrated in Fig. 2. We can forcibly stack the photoresist to 180 μm height by spin-coating two times and to 250 μm by three iterations of spin-coating, where the radial dimension matches with microvasculature. Through the conventional photolithography procedure, rectangular resist patterns could be obtained with 233 μm width and 148 μm height (Fig. 2a). Due to the abnormally high stacking of the positive photoresist, the initial shape was undesirable and the side face was shrunk. However, those patterns were converted into cylindrical micropatterns by a reflow phenomenon when heated at 105 °C. The initial 2-min baking process caused the rectangular pattern to melt into a wider form, resulting in an ellipse shape (Fig. 2b). After 3 min, the pattern tended to change into an incomplete half-circular shape (Fig. 2c), and further baking for 5 min led to the convex circular shape of the thick positive photoresist (Fig. 2d). As the solvent in the resist was evaporated, the dimension of the circular microchannel was gradually constricted, thereby resulting in a final diameter of 230 μm. For a quantitative analysis of the reflow phenomenon depending on heating time, we calculated the aspect ratio of the resist patterns by measuring the width (the major axis of the ellipse) and height (from the major axis of the ellipse to the top) (Fig. S1). Since the major axis of the ellipse was relatively larger than the height after 2 min, the ratio value was 0.25. This ratio value became ~0.5 after 3 min, but a steady and perfect circular shape was achieved in 5 min. The surface roughness was measured as 0.895 nm as shown in Fig. S2.

Since the reflow phenomenon is mainly governed by the surface tension between the substrate and liquid resist [23–25], surface uniformity of the substrate is essential. Thus, complete cleaning of the Si wafer substrate and a dehydration step should be properly performed to obtain a reproducible half-spherical PDMS microchannel, as shown in Fig. 2e. If the surface cleaning is omitted, a cross-sectional image of the resultant PDMS channel will resemble the curvature of a droplet (Fig. 2f), likely due to increased surface tension derived from the non-uniformity of the substrate. The aspect ratio of the rectangular positive photoresist in Fig. 2a is another factor that influences the cross-sectional shape. If the aspect ratio is smaller than 0.5 in the resist pattern, the critical angle between the substrate and the photoresist becomes smaller, resulting in a flat and oval shaped PDMS microchannel (Fig. 2g). On the contrary, an aspect ratio >0.5 produces an increased critical angle, generating a droplet curvature (Fig. 2f). Adjustment of the aspect ratio close to 0.5 is necessary to obtain a half-circular shape of the photoresist by the reflow phenomenon. The concave circular PDMS microchannel was fabricated through a replica molding process by using the convex circular resist as a template. Two half-circular PDMS layers were carefully aligned and permanently bonded to form a nearly perfect circular microchannel, as shown in Fig. 2h.

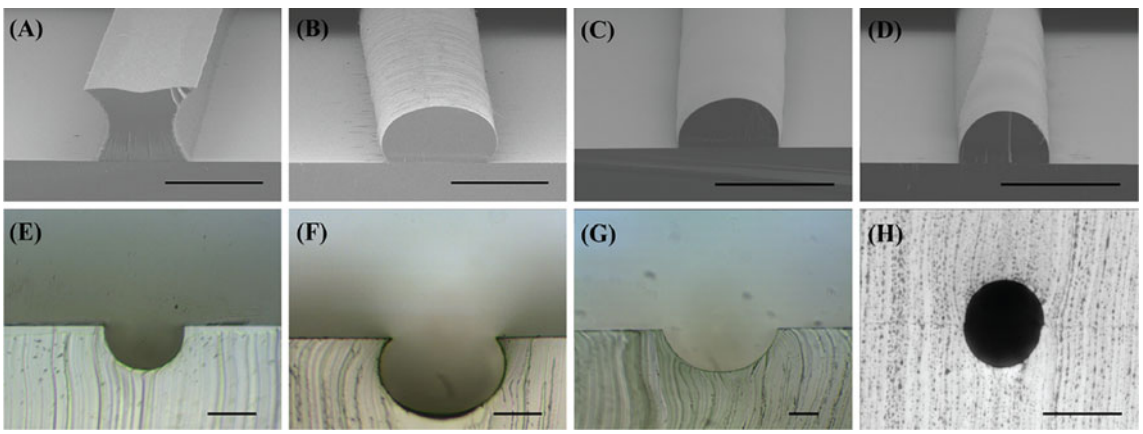

Fig. 2 Reflow phenomenon of positive photoresist as a function of time: **a** 0 min, **b** 2 min, **c** 3 min, and **d** 5 min. The resultant PDMS microchannel by using the half-circular photoresist as a template: the cross-sectional image of **e** the perfect half-circular shape, **f** the droplet shape, **g** ellipse circular shape, and **h** the circular PDMS microchannel. *Scale bars* 200 μm in **a**, **b**, 300 μm in **c**, **d**, and 100 μm in **e**–**h**

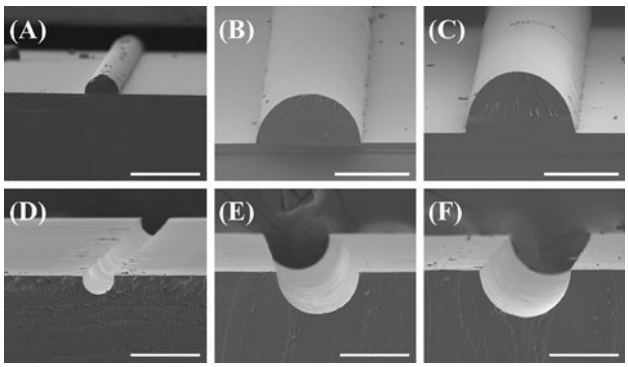

Fig. 3 SEM images of **a–c** the half-circular photoresist, and **d–f** the corresponding half-circular PDMS microchannel. *Scale bars* 200 μm

Fabrication of circular microchannels for constructing a 3D endothelial cell layer

We have focused on mimicking the endothelial cell layer in the microvascular system, where the diameters range from 100 to 400 μm (Fig. S3). Because our approach is based on soft lithography by using a reflow-induced circular photoresist as a template, the tunability of the diameter of the circular channel and a diverse channel route can be easily achieved by controlling the photoresist thickness and through modification of the photomask design. The half-circular micropatterns of the positive photoresist with different diameters and their replication into the PDMS are shown in Fig. 3. We controlled the diameters at 100 (Fig. 3a), 200 (Fig. 3b), and 250 μm (Fig. 3c) by tuning the thickness of the photoresist and the channel width on the mask. Although a previous publication reported on circular polymer microchannels obtained using a negative photoresist, precise controllability over the circular shape was not fully realized, and the diameter of the microchannel was at most 120 μm which has limitations for mimicking in vivo blood vessels [15]. A mechanical micromilling technique enables the creation of a complex 3D circular microchannel with high precision, but it requires expensive metal masters when channel modification is necessary, and accompanies difficulties in forming small diameter capillary microchannels [19]. On the contrary, the proposed technology can produce a circular microchannel based on a simple reflow technique with high tunability of diameters from 100 to 400 μm. By using the convex resist pattern as a template, half-circular PDMS microchannels were accordingly generated through the replica molding technique, and the resultant diameters of 100 (Fig. 3d), 200 (Fig. 3e), and 250 μm (Fig. 3f) precisely matched those of the circular resist.

Since the endothelial cells undergo morphologic differentiation depending on the channel size as well as the structures [26], we mimicked the in vivo system by changing not only the diameters of the microchannels, but also the channel designs. Figure 4 shows various routes of half-circular PDMS microchannels. Straight, S-, X-, cross, Y-, and curve-shapes were patterned on the mask and transferred onto the thick positive photoresist. After the reflow process, the various shapes of the PDMS channel were replicated from the convex circular resist. All the PDMS channels have a half-circular cross-section, and these results imply that the in vivo vascular network can be imitated through a combination of these various routes of circular microchannels. Figure 4g shows the circular microchannel network and the cross-sectional circular shape is still maintained. It is noteworthy that our approach does not require expensive metal molds or complicated fabrication process, but only needs a simple soft lithography and baking process to produce a variety of half-circular microchannels.

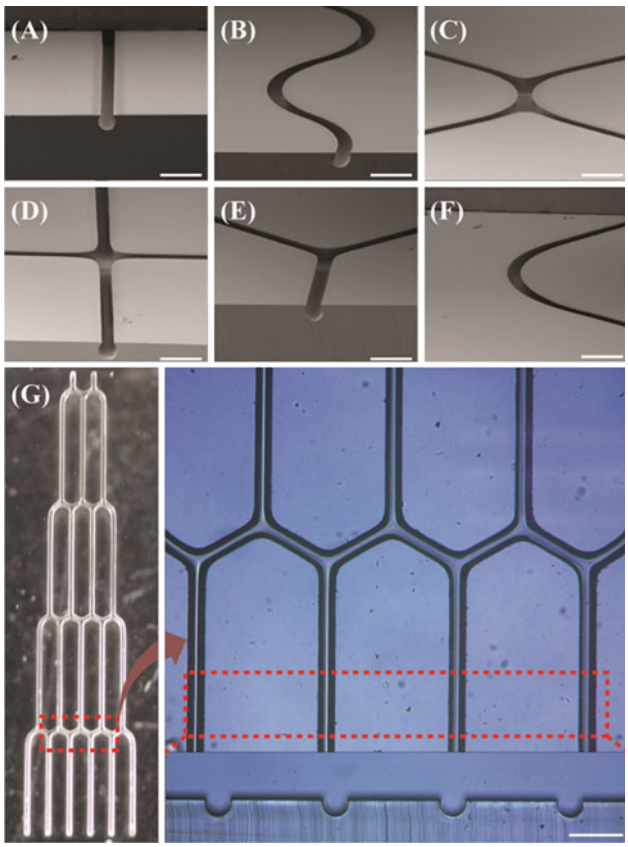

Fig. 4 A variety of channel routes of half-circular PDMS microchannels. **a** straight, **b** S-shape, **c** X-shape, **d** cross-shape, **e** Y-shape, **f** curve-shape, and **g** the network of the circular microchannels

HUVEC culture in the half-circular PDMS microchannel

First, we cultured HUVECs inside the half-circular PDMS microchannels and investigated the alignment and morphological response of the endothelial cells. Primary

HUVECs were seeded and cultured for 3 days in the straight, curved, T-, Y-, and cross-patterned microchannels, and then stained with TRITC-labeled phalloidin, which specifically binds to filamentous actins of the cells. As shown in Fig. 5, the HUVECs were cultured and uniformly spread all over the fibronectin-coated half-circular microchannels, and the cells were well aligned along straight (Fig. 5a), curved (Fig. 5b), T-shape (Fig. 5c), Y-shape (Fig. 5d), and cross-shape (Fig. 5e) channel patterns, respectively. In particular, the filamentous actins of the cells attached on the junction regions of the T- and Y-shape channels showed stretchability toward the branches of the channels, suggesting that HUVECs can moderate their fine attachment according to the channel routes. The cross-sectional fluorescence image in Fig. 5f demonstrated that HUVECs are well attached to the half-circular channel. To investigate the 3D cellular morphology and the surface texture, a SEM image for HUVECs attached on the circular microchannel was obtained. The SEM image in Fig. 6a displays high coverage of HUVECs on the circular microchannel wall and tightly packed cell population on the entire area. Note that the cell coverage (1.6×10^5 cells/cm^2) on the curvature microchannel (Fig. 6b) was similar to that of the flat surface (Fig. 6c). These results demonstrate the success of the HUVEC culture on the half-circular microchannel and point toward high potential for constructing a biomimetic microvascular network.

Construction of a 3D endothelial cell layer inside the circular microchannel

We bonded the half-circular microchannels with careful alignment to produce a complete circular PDMS microchannel, and cultured the HUVECs inside the microchannel. To ensure entire cell coverage, we seeded the cells up and down twice into the channel, as described in "Materials and methods" section. Phase contrast images indicating the progress of cell attachment during 24 h are presented in Fig. 7a. The initial round shape of the cells was changed into an elongated morphology after 2 h and the cells then gradually spread over the channel surface after 24 h. The fluorescent staining for filamentous actins in Fig. 7b (top panel) revealed filamentous actins aligned along the channel direction, while the nuclei staining (Fig. 7b, middle panel) shows a large population of HUVECs occupied the whole channel, indicating successful primary HUVECs culture in the circular PDMS microchannel. The cell viability was also confirmed by a live and dead cell assay after 3 day culture. As shown in Fig. 8a (live cell image) and Fig. 8b (dead cell image), more than 99 % of cells were alive even after 3 days in the circular channel, suggesting a high possibility of providing an artificial blood vessel-based bioassay platform. The HUVEC cell coverage on the microchannel was calculated to be about 74 %. To visualize the live HUVEC adhesion in the entire conditions of the circular microchannel, we used a z-stack confocal microscopy evaluation. The tilted and front images of the 3D z-stack (Fig. 8c, d) show that the endothelial cells formed a hollow tube structure inside the microchannel. The rotation of the z-stack projection confirmed the circular endothelial cell monolayer along the microchannels (see animation in the Supplemental material). A side view of the top and

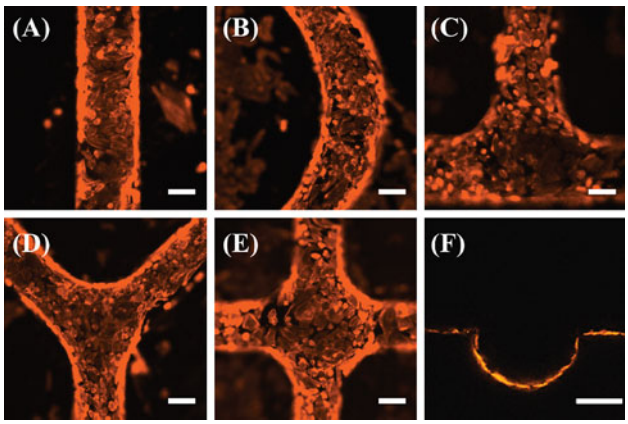

Fig. 5 Primary HUVECs were cultured in the various shaped half-circular PDMS microchannels for 3 days and stained with phalloidin to image filamentous actins of the cells. **a** straight, **b** curved, **c** T-shape, **d** Y-shape, and **e** cross-shape. **f** The cross-sectional fluorescence image of the cultured cells in the half-circular microchannel. *Scale bars* 100 μm

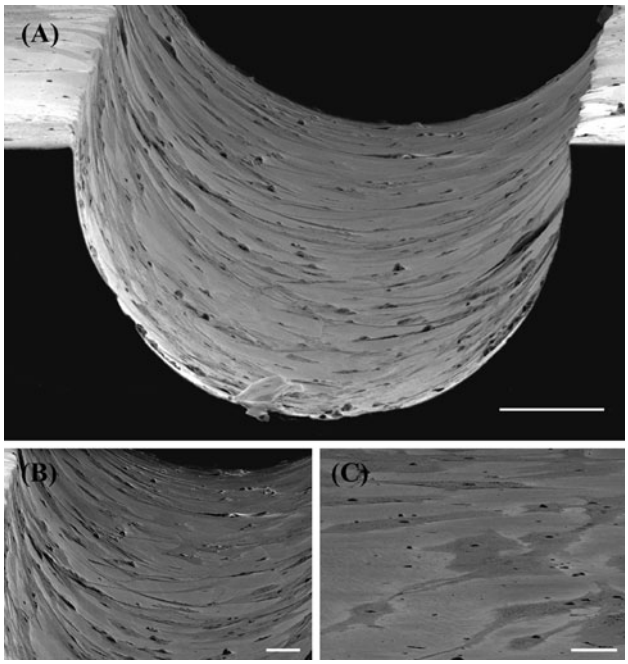

Fig. 6 **a** SEM image of HUVECs attached to the circular PDMS microchannel, and **b** the zoom-in image. **c** HUVECs attached on the flat PDMS surface. *Scale bars* 50 μm in **a**, 20 μm in **b** and **c**

bottom layers of the microdevice was also visualized, as shown in Fig. 8e, displaying a uniform cell attachment along the microchannel wall.

Shear stress on the endothelial cells in the microfluidics influences the cell adhesion, gene expression, cell migration and alignment [27–32]. To confirm steady HUVEC attachment on the microchannel surface, we introduced a medium solution with a flow rate of 1.4 μL/s, which induces high shear stress similar to that in an artery [33]. The shear stress τ (dyn/cm^2) in the circular microchannel is expressed as:

$$\tau = 32\eta Q/[\pi D^3], \quad (1)$$

where η is the viscosity of the medium, Q is the fluid flow rate, and D is the diameter of a circular microchannel. Here, η was approximated as the viscosity of water at 37 °C (0.007 dyn s/cm^2). τ was calculated as 12.48 dyn/cm^2 from Eq. (1). The endothelial cell layer was maintained under this high shear stress for 2 h, and the time-course cell response observed, revealing that the cell density underwent little change (Fig. S4). In addition, the morphology response of the HUVECs to shear stress was quantitatively evaluated in terms of the angle orientation and the shape index (SI) [34]. The angle orientation was defined as the angle between the cell's major axis and the flow direction, ranging from 0° (a cell perfectly aligned with the direction of flow) to 90° (a cell perpendicular to the direction of flow). The SI is defined as:

$$\mathrm{SI} = 4\pi A/P^2, \quad (2)$$

where A is the area of the cell and P is the perimeter of the cell. The SI ranges from 0 (a straight line) to 1 (a perfect circle), which indicates the degree of elongation of a cell. As shown in Fig. S4(B) and S4(C), HUVECs in the microfluidic channel did not exhibit a significant decrease in the angle of orientation or the SI after being exposed to high shear stress for 2 h. These results suggest that the cultured HUVECs in the circular microchannel can be firmly attached even at high shear stress of physiological in vivo level, and indicate strong potential for constructing a microvascular system in circular microfluidics.

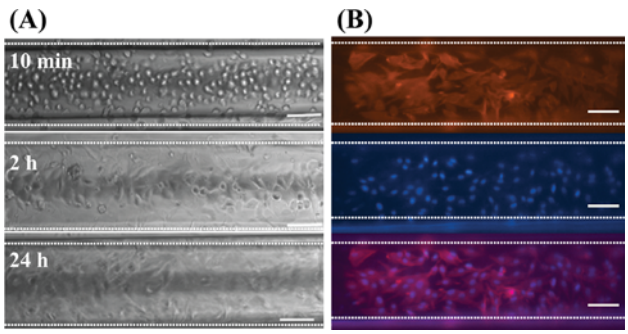

Fig. 7 HUVEC culture in the complete circular microchannel. **a** Time-dependent cell attachment profiles after introducing into the fibronectin-coated circular PDMS microchannel. **b** Fluorescence staining images of the filamentous actins (*top panel*), nuclei (*middle panel*), and their merged image (*bottom panel*). *Scale bars* 100 μm

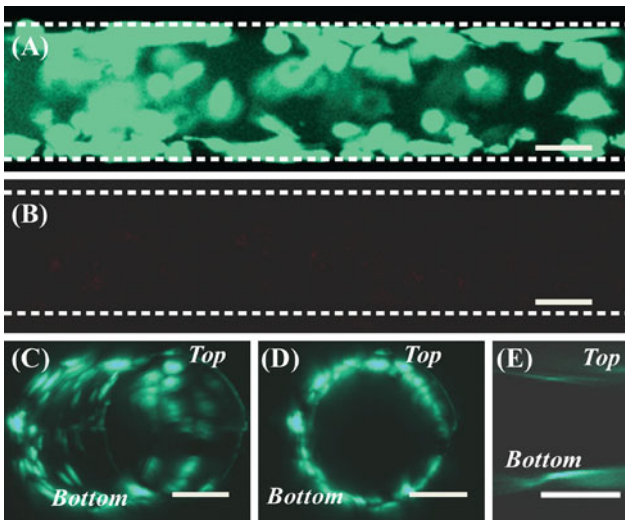

Fig. 8 Live and dead cell assay of HUVECs cultured in the circular microchannel for 3 days. **a** *Green* fluorescence image for the live cells, and **b** *red* fluorescence image for the dead cells. **c** Tilted and **d** front view of the 3D z-stack image for the live HUVECs which were adherent on the entire circular PDMS microchannel. **e** Side view of the top and bottom layer of the HUVECs in the microdevice. *Scale bars* 100 μm (colour figure online)

Conclusions

We have developed an efficient fabrication method for generating a nearly perfect circular PDMS microchannel to mimic the artificial blood vessel system. Our novel approach is based on soft lithography combined with a thick photoresist reflow phenomenon, and we could thereby tune the diameter of the circular channel as well as the channel routes with ease to form the microvascular structure. Furthermore, we successfully cultured the primary HUVEC inside the circular PDMS microchannel with 74 % coverage, and demonstrated cell alignment along the channel direction and cell viability after 3 days. These in vivo-like cell microdevices could provide a more reliable and practical platform than the conventional 2D-based cell assays in the fields of drug screening and chemical/biological diagnostics.

Acknowledgments This research was supported by the Converging Research Center Program funded by the Ministry of Education, Science and Technology (2011K000864), and the Advanced Biomass R&D Center (ABC) of Global Frontier Project funded by the Ministry of Education, Science and Technology (2011-0031357).

References

1. Auroux PA, Iossifidis D, Reyes DR, Manz A (2002) Anal Chem 74:2637–2652
2. Takayama S, Ostuni E, LeDuc P, Naruse K, Ingber DE, Whitesides GM (2001) Nature 411:1016
3. Lucchetta EM, Lee JH, Fu LA, Patel NH, Ismagilov RF (2005) Nature 434:1134–1138
4. Dittrich PS, Manz A (2006) Nat Rev 5:210–218
5. Kang L, Chung BG, Langer R, Khademhosseini (2008) Drug Discov Today 13:1–13
6. Wu MH, Huang SB, Lee GB (2010) Lab Chip 10:939–956
7. Kvietys PR, Granger DN (1997) Am J Physiol Gastrointest Liver Physiol 273:G1189–G1199
8. Young EW, Simmons CA (2010) Lab Chip 10:143–160
9. Ades EW, Candal FJ, Swerlick RA, George VG, Summers S, Bosse DC, Lawley TJ (1992) J Invest Dermatol 99:683–690
10. Gerritsen ME (1987) Bioichem Pharmacol 36:2701–2711
11. Lee JS (2000) Ann Biomed Eng 28:1–13
12. Wang GJ, Lin YC, Hsu SH (2010) Biomed Microdevices 12:841–848
13. Borenstein JT, Tupper MM, Mack PJ, Weinberg EJ, Khalil AS, Hsiao J, Garcia-Cardena G (2010) Biomed Microdevices 12:71–79
14. Becker H, Locascio LE (2002) Talanta 56:267–287
15. Wang GJ, Ho KH, Hsu SH, Wang KP (2007) Biomed Microdevices 9:657–663
16. Grosse A, Grewe M, Fouckhardt H (2001) J Micromech Microeng 11:257–262
17. Yang LJ, Chen YT, Kang SW, Wang YC (2004) Int J Mach Tool Manu 44:1109–1114
18. Futai N, Gu W, Takayama S (2004) Adv Mater 16:1320–1323
19. Wilson ME, Kota N, Kim Y, Wang Y, Stolz DB, LeDuc PR, Ozdoganlar OB (2011) Lab Chip 11:1550–1555
20. Song SH, Lee CK, Kim TJ, Shin IC, Jun SC, Jung HI (2010) Microfluid Nanofluid 9:533–540
21. Fiddes LK, Raz N, Srigunapalan S, Tumarkan E, Simmons CA, Wheeler AR, Kumacheva E (2004) Biomaterials 31:3459–3464
22. Lee SH, Kang DH, Kim HN, Suh KY (2010) Lab Chip 10:3300–3306
23. O'Neill FT, Sheridan JT (2002) Optik 113:391–404
24. Bauer J, Drescher G, Illig M (1996) J Vac Sci Technol B 14:2485–2492
25. Voinov OV (1999) J Appl Mech Tech Phys 40:86–92
26. Kubota Y, Kleinman HK, Martin GR, Lawley TJ (1988) J Cell Biol 107:1589–1598
27. Young EW, Wheeler AR, Simmons CA (2007) Lab Chip 7:1759–1766
28. Tanaka Y, Kikukawa Y, Sato K, Sugii Y, Kitamori T (2007) Anal Sci 23:261–266
29. Khan OF, Sefton MV (2011) Biomed Microdevices 13:69–87
30. Hsu S, Thakar R, Liepmann D, Li S (2005) Biochem Biophys Res Commun 337:401–409
31. Li S, Chen BP, Azuma N, Hu YL, Wu SZ, Sumpio BE, Shyy JY, Chien S (1999) J Clin Invest 103:1141–1150
32. Shiu YT, Li S, Marganski MA, Usami S, Schwartz MA, Wang YL, Dembo M, Chien S (2004) Biophys J 86:2558–2565
33. Ku DN, Giddens DP, Zarins CK, Glagov S (1985) Arterioscler Thromb Vasc Biol 5:293–302
34. Song JW, Gu W, Futai N, Warner KA, Nor JE, Takayama S (2005) Anal Chem 77:3993–3999